Finite Element Modeling of Heat and Moisture Transfer in Porous Material

V. D. Thi, M. Li, M. Khelifa, M. El Ganaoui, Y. Rogaume

Abstract—This paper presents a two-dimensional model to study the heat and moisture transfer through porous building materials. Dynamic and static coupled models of heat and moisture transfer in porous material under low temperature are presented and the coupled models together with variable initial and boundary conditions have been considered in an analytical way and using the finite element method. The resulting coupled model is converted to two nonlinear partial differential equations, which is then numerically solved by an implicit iterative scheme. The numerical results of temperature and moisture potential changes are compared with the experimental measurements available in the literature. Predicted results demonstrate validation of the theoretical model and effectiveness of the developed numerical algorithms. It is expected to provide useful information for the porous building material design based on heat and moisture transfer model.

Keywords—Finite element method, heat transfer, moisture transfer, porous materials, wood.

Nomenclature

c_m [kg/(kg.°M)]	moisture storage capacity
c_p [J/(kg.K)]	specific heat
D_m[kg/(m.s.°M)]	moisture diffusion coefficient
H [m]	height of specimen
h_C [W/(m^2.K)]	convective heat transfer coefficient
h_m [kg/(m^2.s.°M)]	convective moisture transfer coefficient
h_{LV} [kJ/kg]	heat of phase change
L [m]	thickness of specimen
M [kg/kg]	moisture content
m [°M]	moisture potential
T [K]	temperature
t [s]	time
x [m] and y [m]	location coordinates
x_1 [m]	inner distance
x_2 [m]	outer distance
ε	ratio of vapor diffusion coefficient to coefficient of total moisture diffusion
λ [W/(m.K)]	thermal conductivity
δ [kg$_{moisture}$/(kg.K)]	thermal gradient coefficient
ρ [kg/m^3]	dry solid density
γ [J/kg]	latent heat
in	inner reference
out	outer reference
0	initial
∞	ambient atmosphere

Van Diem Thi, Mengya Li, Mohammed El Ganaoui, and Yann Rogaume are with the University of Lorraine, LERMAB, EA 4370, IUT de Longwy, 54400 Cosnes et Romain, France.

Mourad Khelifa is with the University of Lorraine, LERMAB, EA 4370, 27 rue Philippe Séguin, CS 60036, 88026 Epinal, Cedex, France, (e-mail: mourad.khelifa@univ-lorraine.fr).

I. Introduction

THE behavior of porous building material such as wood subjected to different environmental conditions is highly dependent on its material structure and chemical composition. The quantity of water inside wood affects its thermo-physical properties and geometric shape. Being porous, hygroscopic and orthotropic material, the heat and moisture transfer in timber makes a complex system of coupled mechanisms. Moreover, if the moisture content changes over time, this may induce distortions, residual stresses, and failures in timber products. In this case, almost all properties in wood as well as the wood–water relations are temperature-dependent. For these reasons, it is of particular interest to have well knowledge of these variables in various timber structures. The main objective of this article is to achieve an analysis of the heat and moisture transfers in porous materials by means of coupled model adopted for finite element analysis.

In the last decades, to improve building energy efficiency and indoor air quality, the coupled heat and moisture transfers in porous materials have been widely studied due to its presence in many industrial applications. Particularly in timber building, researches have been performed [1]-[3]. To evaluate coupled heat and moisture transfer in porous building materials, Abahri et al. proposed a one-dimensional model [1]. For the numerical models, it was found that the comparisons with experimental results give a good correspondence between the distribution of temperature and moisture content inside the porous slab. Chang et al. also described an analytical solution to coupled heat and moisture diffusion transfer in porous materials. For the same application, the obtained results for the wooden slab are similar with published analytical solutions using the decoupling technique [2]. In [3], Younsi et al. present a mathematical model based on a set of coupled, heat and mass transfer equations presented by Luikov [4]. They have also studied the effect of heat and mass transfer parameters through the Biot number on heat and moisture transfer. It was concluded that the governing dimensionless parameters have a significant influence on the kinetics of the heat and moisture transfer. To analyze the heat and moisture transfers in capillary porous media, Luikov [5] proposed a model assuming the same analogy between moisture transport and heat transfer. This model was used by several researchers [6], [7].

To solve the obtained coupled system for temperature and moisture potentials, many authors used both theoretical and numerical approaches. The solution of the governing partial differential equations depends on the considered specific problem. Generally, all approaches are based on the use of

World Academy of Science, Engineering and Technology
International Journal of Materials and Metallurgical Engineering
Vol:11, No:4, 2017

transformation functions. Chang et al. [3] have introduced a potential function corresponding to their equations system, using a change of variables for temperature gradient and moisture rate. They used the boundary condition of Neumann type and compared their predicted results with those of Thomas et al. [8]. This paper presents a numerical strategy applied to solve the partial differential equations. It concerns two-dimensional heat and moisture transfer through porous building materials. The finite element solutions were performed using two different boundary conditions. Natural hygrothermal boundary conditions proposed by Chang et al. [2] and non-symmetric Dirichlet boundary conditions developed by Abahri et al. [1] are considered. A numerical approach by means of incremental finite element method will be presented. In order to validate the proposed finite element model, a numerical procedure and a staggered technique to resolve the coupling between temperature and moisture are given in details. Moreover, the comparisons of the obtained numerical results with other models given by Abahri et al. [1], Chang et al. [2] and Younsi et al. [3] were performed.

II. ANALYTICAL FORMULATION

A. Used Assumptions

A typical heat and moisture transfer problem involves a two-dimensional capillary porous specimen (timber) in local coordinates, initially at uniform temperature and uniform moisture content. The boundaries are in contact with the hot surrounding gas, thus resulting in a convection boundary condition for both the temperature and moisture potential as shown in Fig. 1.
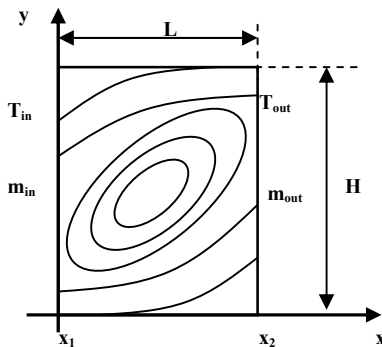

Fig. 1 Coordinate system for porous building material

Heat and moisture transfer in porous media subjected to convective boundary conditions can be modeled using Luikov's approach presented in [5]. The following assumptions are assumed in this work:

- The timber specimen is homogenous and the thermo-physical properties are constant.
- The initial values of moisture and temperature in wood were uniform.
- The shrinkage and the degradation of the timber sample were neglected.

B. Governing Equations

The constitutive equations describing two-dimensional heat and moisture transfer for wood are given by [9] and [10] as:

Heat transfer

$$\rho c_p \frac{\partial T}{\partial t} = \lambda \left(\frac{\partial^2 T}{\partial x^2} + \frac{\partial^2 T}{\partial y^2} \right) + \rho c_m \left(\varepsilon . h_{LV} + \gamma \right) \frac{\partial m}{\partial t} \quad (1)$$

Moisture transfer

$$\rho c_m \frac{\partial m}{\partial t} = D_m \left(\frac{\partial^2 m}{\partial x^2} + \frac{\partial^2 m}{\partial y^2} \right) + \delta . D_m \left(\frac{\partial^2 T}{\partial x^2} + \frac{\partial^2 T}{\partial y^2} \right) \quad (2)$$

$T[K]$ is the temperature, $m[°M]$ is the moisture potential, $t[s]$ is time, $x[m]$ and $y[m]$ are the location coordinates, $c_p[J/(kg.K)]$ and c_m [kg/(kg.°M)] are heat and moisture capacities of the medium, λ [W/(m.K)] and D_m [kg/(m.s.°M)] are thermal and moisture diffusion coefficients respectively, ρ [kg/m³] is the dry solid density, ε is the ratio of vapour diffusion coefficient to coefficient of total moisture diffusion, γ [J/kg] is the latent heat, δ [kg_{moisture}/(kg.K)] is the thermal gradient coefficient and h_{LV} [kJ/kg] is the heat of phase change.

C. Initial and Boundary Conditions

The associated hygrothermal boundary and initial conditions are listed below to complete the numerical formulation of the problem:

1. Non-Symmetric Dirichlet Boundary Conditions Adopted in [1]:

a. Initial Conditions

$$T(x,y,t=0)=T_0; \quad m(x,y,t=0)=m_0 \quad (3)$$

$$T(x=0,y,t)=T_{in}; \quad T(x=L,y,t)=T_{out}$$
$$m(x=0,y,t)=m_{in}; \quad m(x=L,y,t)=m_{out} \quad (4)$$

The moisture potential m is related to the moisture content M by:

$$M=c_m \times m \quad (5)$$

c_m [kg/(kg.°M)] is the specific mass capacity.

b. Boundary Conditions

$$\frac{\partial T}{\partial y}(x,y=0,t)=0; \quad \frac{\partial T}{\partial y}(x,y=H,t)=0 ;$$
$$\frac{\partial m}{\partial y}(x,y=0,t)=0; \quad \frac{\partial m}{\partial y}(x,y=H,t)=0 \quad (6)$$

2. Initial and Boundary Conditions Adopted in [2]

To apply the same boundary conditions assumed in [2], we consider an infinitely long rectangular plate, having inner and outer distances $x_1[m]$ and $x_2[m]$, respectively, subjected to symmetrical hydrothermal loads.

a. Initial Conditions

$$T(x,y,t=0)=T_0; \quad m(x,y,t=0)=m_0 \quad (7)$$

World Academy of Science, Engineering and Technology
International Journal of Materials and Metallurgical Engineering
Vol:11, No:4, 2017

$$T(x_1,y,t)=T_\infty; \quad T(x_2,y,t)=T_\infty;$$
$$m(x_1,y,t) = m_\infty; \quad m(x_2,y,t) = m_\infty \tag{8}$$

b. Boundary Conditions

$$\lambda\frac{\partial T}{\partial x}(x_1,y,t)=h_C\left[T(x_1,y,t)-T_\infty\right]$$
$$+(1-\varepsilon)h_{LV}h_m\left[m(x_1,y,t)-m_\infty\right] \tag{9}$$

$$\lambda\frac{\partial T}{\partial x}(x_2,y,t)=-h_C\left[T(x_2,y,t)-T_\infty\right]$$
$$-(1-\varepsilon)h_{LV}h_{ml}\left[m(x_2,y,t)-m_\infty\right] \tag{10}$$

$$D_m\frac{\partial m}{\partial x}(x_1,y,t)+\delta D_m\frac{\partial T}{\partial x}(x_1,y,t)=h_m\left[m(x_1,y,t)-m_\infty\right] \tag{11}$$

$$D_m\frac{\partial m}{\partial x}(x_2,y,t)+\delta D_m\frac{\partial T}{\partial x}(x_2,y,t)=-h_m\left[m(x_2,y,t)-m_\infty\right] \tag{12}$$

$$\frac{\partial T}{\partial y}(x,y=0,t)=0; \quad \frac{\partial T}{\partial y}(x,y=H,t)=0;$$
$$\frac{\partial m}{\partial y}(x,y=0,t)=0; \quad \frac{\partial m}{\partial y}(x,y=H,t)=0 \tag{13}$$

h_C [W/(m^2.K)] is the convective heat transfer coefficient and h_m [kg/(m^2.s.°M)] is the convective moisture transfer coefficient.

Equations (1)-(2) are coupled heat and moisture transfer equations for porous building materials can be solved numerically by the finite element modelling.

III. FINITE ELEMENT MODELING

A. Numerical Procedure

The Galerkin's weighted residual method is used to discretise the space for (1) and (2). Temperature T is selected as the state variable for heat transfer. The state variable for moisture transfer is chosen as moisture potential, denoted as m. For an element, the state variables are approximated by linearizing three node elements, for example:

$$T(x,y,t)=\sum_{i=1}^{3}N_i(x,y).T_i(t); \quad m(x,y,t)=\sum_{i=1}^{3}N_i(x,y).m_i(t) \tag{14}$$

where $N_i(x,y)$ is the shape functions of triangular finite element, $T_i(t)$ are the time-dependent nodal temperatures and $m_i(t)$ are the time-dependent nodal moistures. Applying Galerkin's weighted residual approach to (1) and (2):

$$\rho c_p\int_\Omega N_i\frac{\partial T}{\partial t}d\Omega=\lambda\int_\Omega N_i\left(\frac{\partial^2 T}{\partial x^2}+\frac{\partial^2 T}{\partial y^2}\right)d\Omega$$
$$+\rho c_m\left(\varepsilon.h_{LV}+\gamma\right)\int_\Omega N_i\frac{\partial m}{\partial t}d\Omega \tag{15}$$

$$\rho c_m\int_\Omega N_i\frac{\partial m}{\partial t}d\Omega=D_m\int_\Omega N_i\left(\frac{\partial^2 m}{\partial x^2}+\frac{\partial^2 m}{\partial y^2}\right)d\Omega$$
$$+\delta.D_m\int_\Omega N_i\left(\frac{\partial^2 T}{\partial x^2}+\frac{\partial^2 T}{\partial y^2}\right)d\Omega \tag{16}$$

Inserting boundary conditions, applying the phase equilibrium relations and rearranging (15) and (16), the resulting system of ordinary differential equations is obtained:

$$\left[C_T\right]\{\dot{T}\}+\left[K_T\right]\{T\}=\left[F_T\right]\{m\} \tag{17}$$

$$\left[C_m\right]\{\dot{m}\}+\left[K_m\right]\{m\}=\left[F_m\right]\{T\} \tag{18}$$

where $\left[C_T\right],\left[K_T\right],\left[F_T\right],\left[C_m\right],\left[K_m\right]$ and $\left[F_m\right]$ are corresponding matrices consisting of coefficients derived from (15) and (16).

B. Numerical Integration

The coupled response of (17) and (18) may be solved using either the dynamic explicit scheme or the implicit scheme. Using an implicit global resolution scheme, the moisture field derived in the previous time step is first used in the temperature equation (17) and a new temperature field is obtained without changing the moisture. The temperatures obtained are then used in (18) to calculate the new moisture potential.

Evaluating the temperature field and moisture potential at state (n+1) from (17) and (18) using the implicit solution approach described above, we obtain:

$$\left[C_T\right]\{T^{n+1}\}+\Delta t.\left[K_T\right]\{T^{n+1}\}=\Delta t.\left[F_T\right]\{m^{n+1}\}+\left[C_T\right]\{T^n\} \tag{19}$$

$$\left[C_m\right]\{m^{n+1}\}+\Delta t.\left[K_m\right]\{m^{n+1}\}=\Delta t.\left[F_m\right]\{T^{n+1}\}+\left[C_m\right]\{m^n\} \tag{20}$$

$$\{T^{n+1}\}=\left[\left[C_T\right]+\Delta t.\left[K_T\right]\right]^{-1}\left(\Delta t.\left[F_T\right]\{m^{n+1}\}+\left[C_T\right]\{T^n\}\right) \tag{21}$$

$$\{T^{n+1}\}=\left[A_T\right]^{1}\left(\Delta t.\left[F_T\right]\{m^{n+1}\}+\left[C_T\right]\{T^n\}\right) \tag{22}$$

Substituting (22) into (20), we obtain:

$$\left(\left[C_m\right]+\Delta t.\left[K_m\right]\right).\{m^{n+1}\}=\Delta t.\left[F_m\right]\left[A_T\right]^{1}\left(\Delta t.\left[F_T\right]\{m^{n+1}\}+\left[C_T\right]\{T^n\}\right)$$
$$+\left[C_m\right]\{m^n\} \tag{23}$$

$$\left(\left[C_m\right]+\Delta t.\left[K_m\right]-\Delta t^2.\left[F_m\right]\left[A_T\right]^{1}\left[F_T\right]\right).\{m^{n+1}\}=$$
$$\Delta t.\left[F_m\right]\left[A_T\right]^{1}\left[C_T\right]\{T^n\}+\left[C_m\right]\{m^n\} \tag{24}$$

$$\{m^{n+1}\}=\left[A_m\right]^{1}\{B_m\} \tag{25}$$

$$\{T^{n+1}\}=\left[A_T\right]^{1}\{B_T\} \tag{26}$$

where:

$$\left[C_T\right]=\rho c_p\int_\Omega\{N_i\}<N_j>d\Omega \tag{27}$$

World Academy of Science, Engineering and Technology
International Journal of Materials and Metallurgical Engineering
Vol:11, No:4, 2017

$$[K_T]=\lambda\int_\Omega\left[\left\{\frac{\partial N_i}{\partial x}\right\}<\frac{\partial N_j}{\partial x}>+\left\{\frac{\partial N_i}{\partial y}\right\}<\frac{\partial N_j}{\partial y}>\right]d\Omega \qquad (28)$$

$$[F_T]=-D_m\left(\varepsilon.h_{LV}+\gamma\right)\int_\Omega\left[\left\{\frac{\partial N_i}{\partial x}\right\}<\frac{\partial N_j}{\partial x}>+\left\{\frac{\partial N_i}{\partial y}\right\}<\frac{\partial N_j}{\partial y}>\right]d\Omega \qquad (29)$$

$$[C_m]=\rho c_m\int_\Omega\{N_i\}<N_j>d\Omega \qquad (30)$$

$$[K_m]=D_m\int_\Omega\left[\left\{\frac{\partial N_i}{\partial x}\right\}<\frac{\partial N_j}{\partial x}>+\left\{\frac{\partial N_i}{\partial y}\right\}<\frac{\partial N_j}{\partial y}>\right]d\Omega \qquad (31)$$

$$[F_m]=-\delta.D_m\int_\Omega\left[\left\{\frac{\partial N_i}{\partial x}\right\}<\frac{\partial N_j}{\partial x}>+\left\{\frac{\partial N_i}{\partial y}\right\}<\frac{\partial N_j}{\partial y}>\right]d\Omega \qquad (32)$$

$$[A_T]=[C_T]+\Delta t.[K_T] \qquad (33)$$

$$\{B_T\}=\Delta t.[F_T]\{m^{n+1}\}+[C_T]\{T^n\} \qquad (34)$$

$$[A_m]=[C_m]+\Delta t.[K_m]-\Delta t^2.[F_m][A_T]^{-1}[F_T] \qquad (35)$$

$$\{B_m\}=\Delta t.[F_m][A_T]^{-1}[C_T]\{T^n\}+[C_m]\{m^n\} \qquad (36)$$

The known solutions at step (n) are assumed to be independent of iterations. The start vectors are chosen as the values at the last converged state, i.e.

$$\{T^{n+1}\}^{(i)}=\{T^n\}^{(i-1)}+\delta\{T\}^{(i)}$$
$$\{m^{n+1}\}^{(i)}=\{m^n\}^{(i-1)}+\delta\{m\}^{(i)} \qquad (37)$$

The iteration scheme is stopped when the convergence criterion is verified and the next step is computed. The convergence criterion is given by the scalar product as follow:

$$\left\|\{T^{n+1}\}^{(i)}-\{T^n\}^{(i-1)}\right\|\le 10^{-10}$$
$$\left\|\{m^{n+1}\}^{(i)}-\{m^n\}^{(i-1)}\right\|\le 10^{-10} \qquad (38)$$

The above system of equations (19), (20) is solved numerically by using finite element method and a computer program is written in MATLAB environment.

IV. VALIDATION OF THE MODEL

The developed formulation in Section III is used in the finite element method in order to analyze heat and moisture transfer in porous building materials. The results from the calculations will be in the following compared to the experimental tests.

A. Application on a Wood Slab Building Envelope

An application on a wood slab building envelope has been simulated using the material properties given from [1], [2] which are associated to two different boundary conditions described previously in Section II *C* are recapitulated in Table I.

The Finite Element (FE) model of the wood slab of 24×60 mm is modelled by 960 triangular elements consisted of 525 nodes. Figs. 2 and 3 illustrate respectively the temperature and the moisture distribution in wooden slab sample at different times. From Fig. 2, it can be seen that at time t=1000 s, a larger temperature gradient was established on 3/4 width plane of the tested specimen. During a prolonged heat transfer process (Figs. 2 (a)(c)), the temperature distribution evolves rapidly at the beginning and then becomes stable. The temperature difference between the inner region and the outer region decreases more and more. After the heat and moisture transfer in wood slab panel, a moisture gradient was established in response to temperature gradient with maximum moisture potential in the surface region. The moisture content in the outer region decreased from 80 °M moisture potential to around 70 °M at time t = 4000 s (Fig. 3 (c)). We also note that the moisture rate in the centre zone decreased progressively until the moisture potential reaches 70 °M at time t=1000 s (Fig. 3 (b)).

TABLE I
MATERIAL PROPERTIES FOR WOOD

c_m	0.01 kg/(kg.°M)	ε	0.3
c_p	2500 J/(kg.K)	m_0	86 °M
δ	2 °M/K	m_{in}	45 °M
λ	0.65 W/(m.K)	m_{out}	4 °M
ρ	370 kg/m3	h_{LV}	2.5×10^{-9} J/kg
D_m	2.2×10^{-8} kg/(m.s.°M)	γ	0
L	24 mm	T_∞	110 °C
H	60 mm	m_∞	4 °M
T_0	10 °C	h_c	2.25 W/(m^2.K)
T_{in}	60 °C	h_m	2.5×10^{-6} kg/(m^2.s.°M)
T_{out}	110 °C		

Fig. 4 shows the temperature distribution of at the center of wood slab (x=12 mm). It can be seen that the temperature distributions of the three layers during the heat and moisture transfer can be divided in three different phases: I) An initial rising phase of temperature, II) a non-linear rising in temperature at the center of wood panel and III) a quasi-stable phase in temperature at the center of the wall. The FE results are similar to the experimental results of Abahri et al. [1]. From a short time of 690 s, the temperature is stationary and equal to 85.2 °C, which is well predicted by the model.

Fig. 5 shows the comparison between the analytical solution and predicted results of the moisture potential versus time at the center of wood slab. It can be seen that the moisture potential distributions can be separated in three phases: I) An initial slightly linear increasing phase, II) a quasi-stable phase and III) a non-linear decreasing phase. There is a very good correlation between the analytical solution given in [1] and the obtained numerical results. During the heat and moisture transfer in the porous slab, the moisture potential continues to decrease with increase in time, until the end.

For the same example, the moisture evolution at the surface and at the middle of the slab is shown in Fig. 6. It can be seen that the results from the natural hygrothermal boundary

World Academy of Science, Engineering and Technology
International Journal of Materials and Metallurgical Engineering
Vol:11, No:4, 2017

conditions developed by Chang et al. [2] agree well, even though the boundary conditions are different than used by Abahri et al. [1]. With regard to the moisture content profile of the wood slab at the surface and at the middle presented in Fig. 6, a good accuracy of the present model can then be verified by a very small difference around 1% between the predicted and the results obtained by Chang et al. [2].

(a) Time t = 100 s   (b) Time t = 500 s

(c) Time t = 1000 s
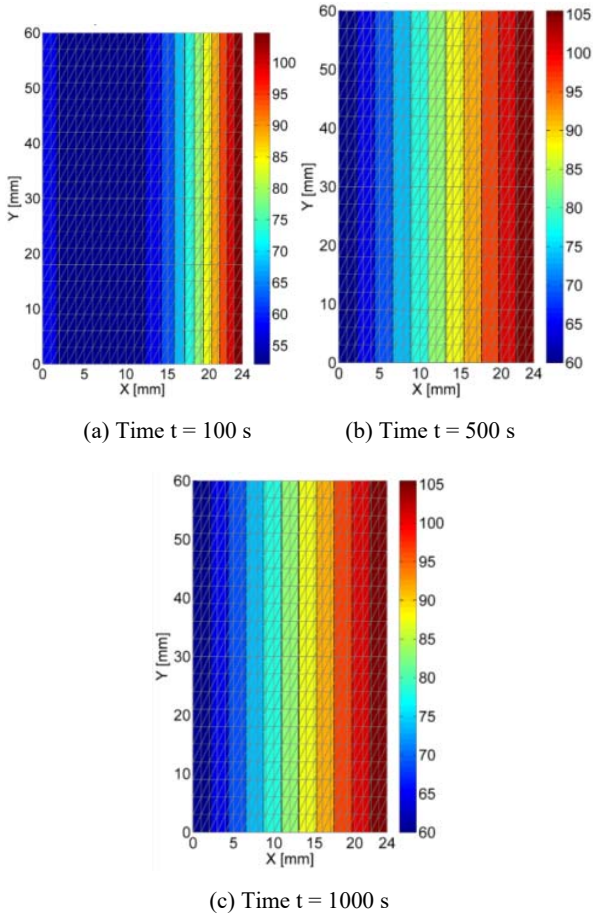
Fig. 2 Contour maps of temperature distribution at different time

(a) Time t = 100 s   (b) Time t = 1000 s

(c) Time t = 4000 s
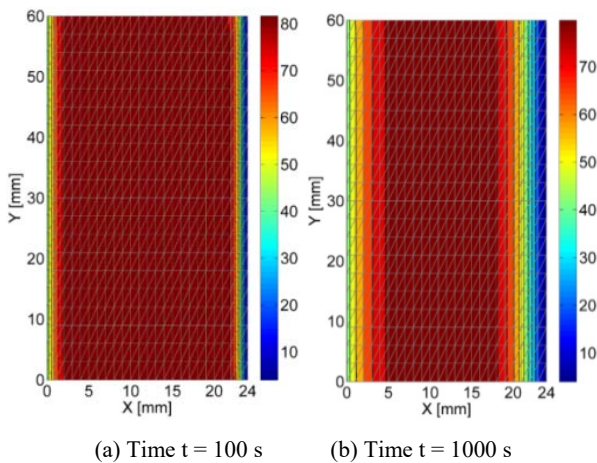
Fig. 3 Contour maps of moisture potential distribution at different time
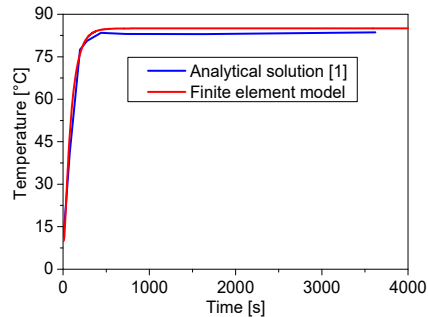
Fig. 4 Curves of temperature versus time at the centre of wood slab
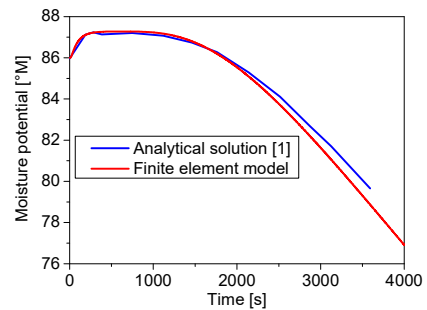
Fig. 5 Curves of moisture potential versus time at the centre of wood slab

The analytical results of the temperature and moisture distributions inside the wood slab are compared with the results obtained by the FE modelling at distinct times, and are illustrated in Figs. 7 and 8, respectively. The transport of capillary water is important in the neighborhood of the inner surface corresponding to the left side of the wood slab. The temperature profile at the center of the panel increases along the time compared to its initial value. This is not the case for the moisture potential value which decreases with time. The maximum differences between the analytical value of the temperature (or moisture potential) and the predicted temperature (or moisture potential) are lower to 0.2%. It can be seen that the FE model shows a good agreement with the analytical model.

World Academy of Science, Engineering and Technology
International Journal of Materials and Metallurgical Engineering
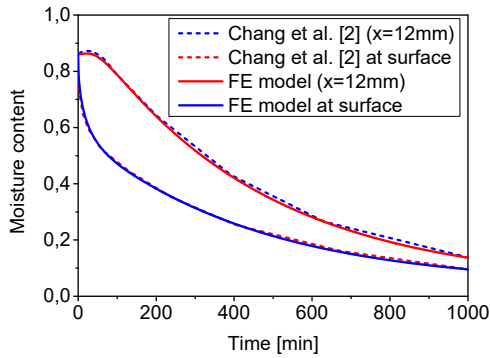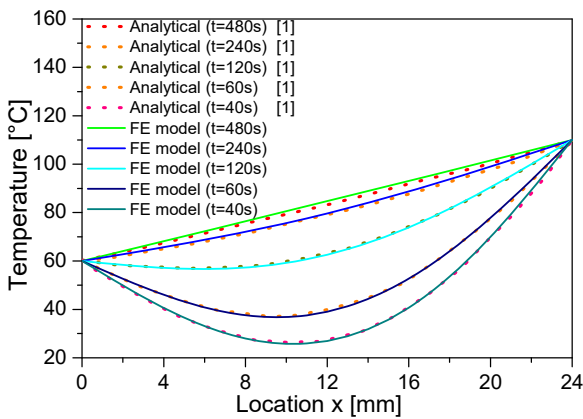Vol:11, No:4, 2017

Fig. 6 Curves of moisture content versus time at two different locations

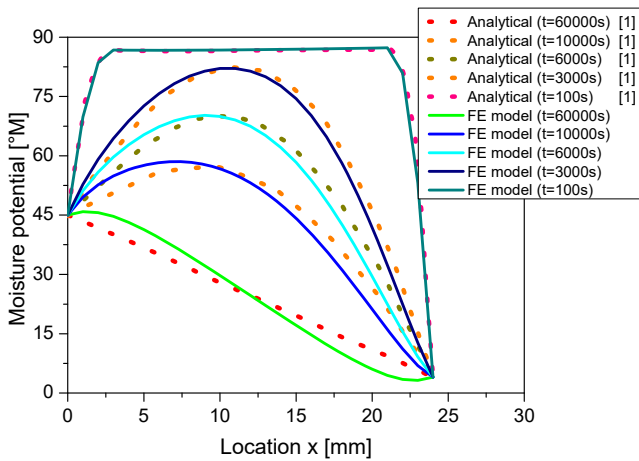Fig. 7 Curves of temperature versus time at the centre of wood slab

Fig. 8 Curves of moisture potential versus time at the centre of wood slab

Due to the dynamical changing of the meteorological parameters, the heat and moisture transfer in the wall building of 0.05 m thickness changes significantly over the period of a day. To study this impact, the meteorological data for one year period of La Rochelle [1] are taken into account in the simulations. The outdoor conditions (solar radiation, outdoor air temperature and outdoor relative humidity) are taken from meteorological data given in [1]. The initial boundary conditions of temperature and moisture content are 10 °C and

50 °M, respectively. The obtained results are given in Fig. 9. During the heating season, as shown in Fig. 9, the fluctuations of the measured temperatures and the moisture contents are slightly smaller than the calculated values. The simulated results also indicate that the coupling term in energy balance equation has no effect on the temperature values because the effect of the involved moisture potential of the porous material which appears in the coupling term of (1) is not significant. The similar results have been found in [1].
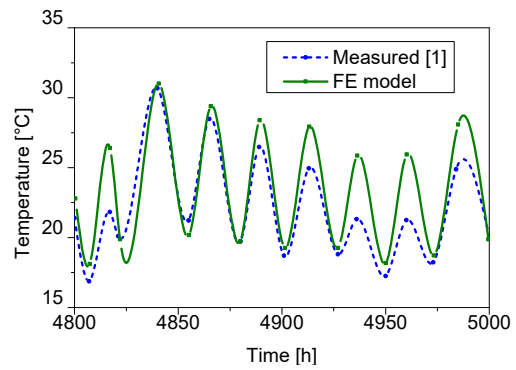
(a) Temperatures
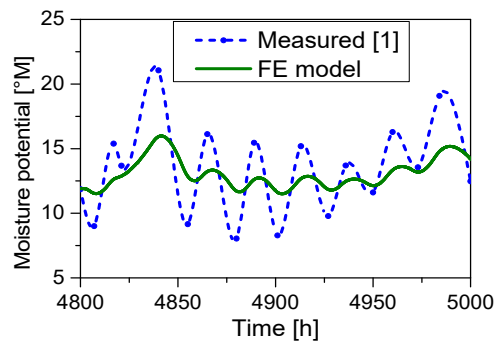
(b) Moisture potentials

Fig. 9 Calculated against measured indoor (a) temperatures and (b) moisture potentials for the porous wall.
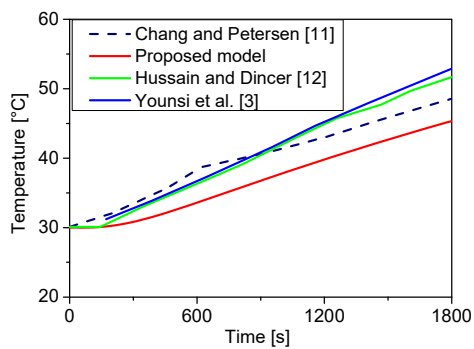
B. Simulation of Heat and Moisture Transfer in Wood Material during Thermal Treatment

The geometrical characteristics of the wood specimen are 48 mm width and 49 mm long. The FE mesh consists of 960 three-node triangular elements. The initial and boundary conditions are recapitulated in Table II to complete the analytical and numerical formulations of this example. The same example was analyzed by Chang and Petersen [11] and Hussain and Dincer [12]. The predicted center temperature and moisture distributions inside the spruce wood panel are compared with experimental data given in [11] and the numerical results presented in [3], [12] and are shown in Fig. 10. A good agreement is found between the predicted results and the experimental data for both models (Luikov model [3] and Diffusion model [12]). The absolute error between numerical results and experimental data is less than 5% for temperature value and less than 3% for moisture content value. Therefore, we can state that the proposed FE model is

World Academy of Science, Engineering and Technology
International Journal of Materials and Metallurgical Engineering
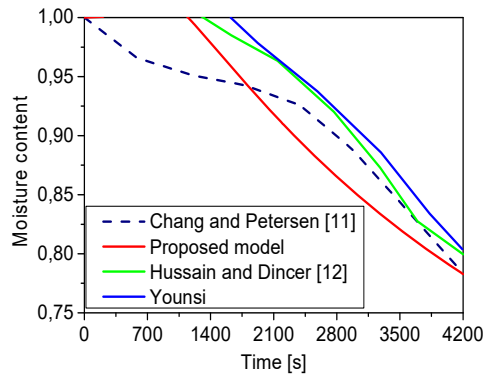Vol:11, No:4, 2017

able to estimate the temperature and moisture content distributions inside the wood samples during thermal treatment.

TABLE II
MATERIAL PROPERTIES FOR SPRUCE WOOD SPECIMEN [3]

c_m	0.01 kg/(kg.°M)	m_0	87 °M
c_p	4201.4 J/(kg.K)	ε	0.3
δ	2 °M/K	h_{LV}	2.5×10^{-9} J/kg
λ	0.577 W/(m.K)	γ	0
ρ	856 kg/m3	T_∞	81 °C
D_m	2.2×10^{-8} kg/(m.s.°M)	m_∞	12 °M
L	49 mm	h_c	25 W/(m².K)
H	48 mm	h_m	10^{-4} kg/(m².s.°M)
T_0	30 °C		

(a) Temperatures

(b) Moisture potentials

Fig. 10 Temperature and moisture content at center of spruce wood sample

V. CONCLUSIONS

The objective of this work is to present a numerical methodology to simulate 2D heat and moisture transfer in porous building materials. In the first step, a generalized mathematical model accounting the governing equations describing the coupled heat and moisture transfers for porous material has been formulated in detail. The associated numerical aspects in the framework of the classical Galerkin-based FE formulation are also discussed. The implicit global resolution scheme as well as the local integration scheme, to compute the values of the temperature and the moisture

content at each integration point of each element, is presented.

Several FE simulations using two different boundary conditions are conducted to compare the predicted results with the analytical and experimental measurements available in literature. The quality of the solutions obtained in terms of the hygrothermal fields' distribution, through the porous panel thickness, seems very satisfactory.

Further investigations are now under progress to extend this numerical procedure to 3D case with the hope of simulating the heat and moisture transfers in the porous building panels made by different materials and several layers under complex and severe hygrothermal conditions.

REFERENCES

[1] Abahri K, Belarbi R, Trabelsi A. Contribution to analytical and numerical study of combined heat and moisture transfer in porous building materials. Build Environ 2011;46:1354-1360.
[2] Chang W, Weng C. An analytical solution to coupled heat and moisture diffusion transfer in porous materials. Int J Heat Mass Tran 2000;43:3621-3632.
[3] Younsi R, Kocaefe D, Kocaefe Y. Three-dimensional simulation of heat and moisture transfer in wood. Appl Therm Eng 2006;26:1274-1285.
[4] Luikov AV. Systems of differential equations of heat and mass transfer in capillary-porous bodies. Int J Heat Mass Tran 1975; 8:1–14.
[5] Luikov AV. Heat and mass transfer in capillary-porous bodies. Oxford: Pergamon Press; 1966. chap. 6.
[6] Thomas HR, Morgan K, Lewis RW. Afully monolinear analysis of heat and mass transfer problems in porous media. Int J Numer Meth Eng 1980;15:1381-93.
[7] Ribeiro JW. Complete and satisfactory solutions of Luikov equations of heat and moisture transport in a spherical capillary-porous body. Int Commun Heat Mass 2000;27:975-84.
[8] Thomas HR, Lewis RW, Morgan K. An application of the finite element method to the drying of timber. Wood Fiber 1980;11(4):237-43.
[9] Liu JY, Cheng S. Solution of Luikov equations of heat and mass transfer in capillary porous bodies. Int J Heat Mass Tran 1991;34:1747-54.
[10] Qin M, Belarbi R. Development of an analytical method for simultaneous heat and moisture transfer in building materials utilising transfer function method. J Mater Civil Eng ASCE 2005;17(5):492-7.
[11] Chiang W.C., Petersen J.N. Experimental measurement of temperature and moisture profiles during apple drying. Dry Technol 1987;5(1):25–49.
[12] Hussain M.M., Dincer I. Numerical simulation of two-dimensional heat and moisture transfer during drying of a rectangular object. Numerical Heat Transfer A 2003; 43:867–878.